Nonlocal Screening of Plasmons in Graphene by Semiconducting and Metallic Substrates: First-Principles Calculations

Jun Yan, Kristian S. Thygesen,* and Karsten W. Jacobsen

Center for Atomic-scale Materials Design, Department of Physics, Technical University of Denmark, DK-2800 Kongens Lyngby, Denmark

(Received 15 October 2010; published 5 April 2011)

We investigate the role of substrates on the collective excitations of graphene by using a first-principles implementation of the density response function within the random-phase approximation. Specifically, we consider graphene adsorbed on SiC(0001) and Al(111) as representative examples of a semiconducting and metallic substrate. On SiC(0001), the long wavelength π plasmons are significantly damped although their energies remain almost unaltered. On Al(111), the long wavelength π plasmons are completely quenched due to the coupling to the metal surface plasmon. The strong damping of the plasmon excitations occurs despite the fact that the single-particle band structure of graphene is completely unaffected by the substrates illustrating the nonlocal nature of the effect.

DOI: 10.1103/PhysRevLett.106.146803 PACS numbers: 73.20.Mf, 73.21.−b, 78.20.Bh

Recent years have witnessed an explosion in the interest for graphene, both as a novel material for technological applications and as a model system for exploring new fundamental physics [1]. As a two-dimensional, half-metallic crystal, graphene exhibits many peculiar properties, in particular, related to its electronic structure. The intrinsic π and σ plasmons of graphene [2–6] as well as the 2D metallic plasmons arising from doping [7,8] and their interactions with electron-hole excitations [9,10] and phonons [11] have been studied both theoretically and experimentally. Besides understanding the elementary excitations, there have been recent attempts to use graphene for nanoplasmonics [12], an emerging field with one of the aims being to develop plasmon-enhanced imaging and sensing techniques [13].

Experimentally, single layers of graphene can be synthesized by various techniques, such as exfoliation of graphite or decomposition of hydrocarbons on transition metal surfaces [14,15]. Wafer sizes of graphene can be grown on SiC substrates by sublimation of Si [16]. For many applications of graphene, in particular, within electronics, the substrate is likely to play an important role and thus should be considered as part of the device. While the effect of substrates on the atomic structure and single-particle excitations of graphene has been studied by using *ab initio* methods [17–20], their influence on the collective electronic excitations has so far been studied only by using dielectric models [21,22].

In this Letter, we present a first-principles study of the effect of substrates on the plasmon excitations in graphene. We concentrate on weakly bound systems in which the atomic structure and the single-particle band structure of graphene are well preserved. In particular, a semiconducting SiC(0001) surface with Si termination, which offers direct comparison with existing measurements [3–6], and a metallic Al(111) surface are discussed here. Our results demonstrate that, even for these weakly coupled systems, the substrate has a profound influence on the plasmonic excitations. For the semiconducting substrate, the π plasmons are strongly damped but still visible, while for the metallic substrate, the π plasmons are completely quenched by coupling to the surface plasmons of the substrate. We find that the electronic response function of the coupled systems can be reproduced from the response functions of the isolated graphene and substrate, showing that the damping of plasmons is controlled by long range Coulomb interactions.

The plasmon excitations are obtained as peaks in the electron energy loss spectrum (EELS) which in turn is related to the linear density response function. For periodic systems, the latter is conveniently calculated in a plane-wave representation $\chi_{\mathbf{GG}'}(\mathbf{q}, \omega)$ by solving a Dyson-like equation

$$\chi_{\mathbf{GG}'}(\mathbf{q}, \omega) = \chi^0_{\mathbf{GG}'}(\mathbf{q}, \omega) + \sum_{\mathbf{G}_1\mathbf{G}_2} \chi^0_{\mathbf{GG}_1}(\mathbf{q}, \omega) K_{\mathbf{G}_1\mathbf{G}_2}(\mathbf{q}) \chi_{\mathbf{G}_2\mathbf{G}'}(\mathbf{q}, \omega), \quad (1)$$

where $\mathbf{G}$ stands for the reciprocal lattice vectors and $\mathbf{q}$ for wave vectors restricted to the irreducible Brillouin zone only. The Coulomb kernel $K_{\mathbf{G}_1\mathbf{G}_2}(\mathbf{q})$ is $4\pi\delta_{\mathbf{G}_1\mathbf{G}_2}/|\mathbf{q} + \mathbf{G}_1|^2$, and the exchange-correlation kernel is neglected within the random-phase approximation employed in the present work. The noninteracting density response function is given by the Adler-Wiser formula [23,24]

$$\chi^0_{\mathbf{GG}'}(\mathbf{q}, \omega) = \frac{1}{\Omega} \sum_{\mathbf{k}}^{\mathrm{BZ}} \sum_{n,n'} \frac{f_{n\mathbf{k}} - f_{n'\mathbf{k}+\mathbf{q}}}{\omega + \epsilon_{n\mathbf{k}} - \epsilon_{n'\mathbf{k}+\mathbf{q}} + i\eta} \times \langle \psi_{n\mathbf{k}} | e^{-i(\mathbf{q}+\mathbf{G})\cdot\mathbf{r}} | \psi_{n'\mathbf{k}+\mathbf{q}} \rangle \times \langle \psi_{n'\mathbf{k}+\mathbf{q}} | e^{i(\mathbf{q}+\mathbf{G}')\cdot\mathbf{r}} | \psi_{n\mathbf{k}} \rangle. \quad (2)$$

The occupation $f_{n\mathbf{k}}$, Kohn-Sham eigenvalue $\epsilon_{n\mathbf{k}}$, and wave function $\psi_{n\mathbf{k}}$ for band n at wave vector $\mathbf{k}$ are extracted from ground state calculations performed with the GPAW code [25,26], a real space implementation of the projector augmented wave method [27].

After obtaining the $\chi_{\mathbf{GG}'}$ matrix, the loss function is calculated as

$$-\mathrm{Im}\epsilon^{-1}(\mathbf{q},\omega) = -\frac{4\pi}{|\mathbf{q}|^2}\,\mathrm{Im}\chi_{\mathbf{G}=0,\mathbf{G}'=0}(\mathbf{q},\omega), \quad (3)$$

which is directly comparable to the EELS measured in experiments. For surface excitations, a surface loss function is defined as [28,29]

$$g(\mathbf{q},\omega) = -\frac{2\pi}{|\mathbf{q}|}\iint dz dz' \chi_{\mathbf{G}_\parallel=\mathbf{G}'_\parallel=0}(z,z';\mathbf{q},\omega)e^{|\mathbf{q}|(z+z')}, \quad (4)$$

where $\parallel$ and z correspond to directions parallel and perpendicular to the surface, respectively; $\chi_{\mathbf{G}_\parallel\mathbf{G}'_\parallel}(z,z';\mathbf{q},\omega)$ is the Fourier transform of $\chi_{\mathbf{GG}'}(\mathbf{q},\omega)$ in the z direction. Details on the numerical implementations, parallelization, and benchmark tests can be found elsewhere [30]. Details on calculation parameters can be found in Ref. [31].

Semiconducting substrate.—The system, shown in Fig. 1(a), consists of two C layers on top of a 4*H*-SiC(0001) surface. The structure is adopted from the literature [17,18], corresponding to a 2×2 unit cell of graphene and four bilayers of SiC as the substrate. Six bilayers of SiC have also been checked and give quantitatively the same spectra for energy below 10 eV. We consider here the combination of the first carbon layer and the SiC surface as the substrate, since they are covalently bonded and the "Dirac cone" band of graphene disappears, leaving a wide energy gap in the band structure shown in Fig. 1(b). The second C layer, which is placed in the graphite-type *AB* stacking order above the first C layer, is treated as the graphene layer. It binds weakly to the first C layer [17,18] in agreement with experiments [32], with a local-density approximation binding energy per C atom of 0.039 eV and adsorption distance of 3.56 Å. As shown in Fig. 1(c), a linear conic band structure appears within the band gap, resembling that of freestanding graphene (red dotted line). The Fermi level is shifted by 0.05 eV above the Dirac point, indicating slight electron doping into this C layer.

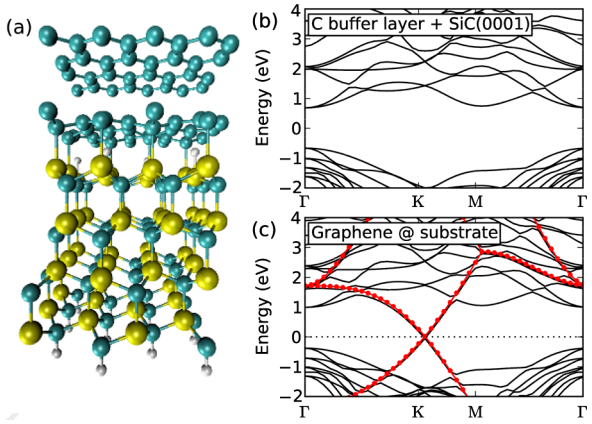

FIG. 1 (color online). (a) Geometry of two carbon (blue) layers on a Si (yellow)-terminated 4*H*-SiC (0001) surface. The dangling bonds are saturated with hydrogen atoms (gray). (b) Band structure of the first carbon buffer layer on the SiC surface. (c) Band structure for the geometry shown in (a) (black solid lines) and for a freestanding graphene (red dotted lines). The dashed line indicates the Fermi level.

Figure 2(a) shows the calculated loss function of freestanding graphene for different $\mathbf{q}$. These spectra are in good agreement with previous *ab initio* calculations [2,10]. The peak around 5 eV corresponds to the π plasmon resonance, and the shoulder below 5 eV originates from the $\pi \rightarrow \pi^*$ single-particle excitations [10]. The energy dispersion relation of these π plasmons is shown in Fig. 2(c) as the red filled dots. Again, they compare well with previous *ab initio* results on freestanding graphene [2]. These π plasmons exhibit a unique quasilinear dispersion, distinct from the parabolic dispersion in graphite [33]. Such a linear relation is attributed to the local field effect, which mixes the electronic transitions from π to π^* band with those around the Dirac cone [2]. Shown in Fig. 2(c) as black filled squares, the SiC substrate has little effect on the energies of these π plasmons. There is only a slight redshift in the plasmon energy for $q < 0.3/\text{Å}$. The overall linear dispersion is well preserved and agrees well with EELS experiments on single-walled nanotubes [2] and SiC(0001) supported graphene [5].

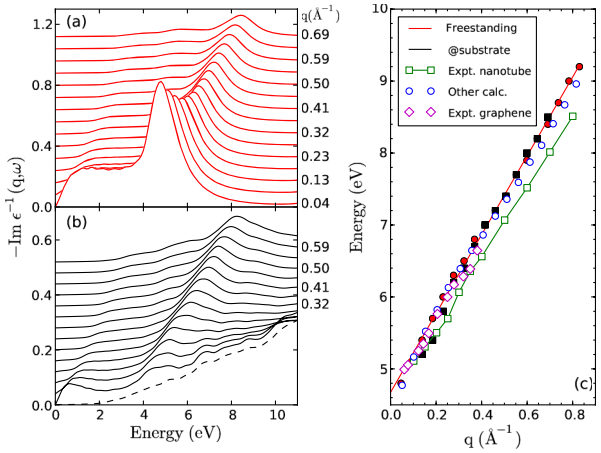

FIG. 2 (color online). Loss function of freestanding graphene (a) and graphene on a SiC substrate (b) as a function of q. The loss functions, from bottom to top (solid lines), correspond to increasing q at an interval of 0.046/Å. The dashed line corresponds to the loss function of the substrate at $q = 0.092/\text{Å}$. (c) Dispersion relations for the π plasmons of freestanding graphene (red filled circles) and graphene on SiC (black filled squares). They are compared with an earlier *ab initio* calculation on freestanding graphene (blue hollow circles) and experiments on single wall carbon nanotubes (green hollow squares) [2] as well as experiments on graphene/SiC(0001) (purple hollow diamonds) [5]. Lines are added to guide the eye.

In contrast, the line shape and strength of the loss function, as shown in Fig. 2(b), are significantly changed by the substrate, especially for small q. At $q = 0.046/\text{Å}$ (the bottom solid line), the π plasmon exhibits a broad binodal structure and its strength reduces to around $1/5$ of that for freestanding graphene. Besides the 5 eV peak, a peak between 0 and 1 eV and a broad band from 6 to 12 eV are also visible in the spectrum. The broad band between 6 and 12 eV comes mainly from the substrate electronic excitations, whose loss function is shown as the dashed line for $q = 0.092/\text{Å}$ for comparison. The peak at around 0.6 eV is the so-called "2D-sheet plasmon" [7,8], which originates from the collective excitations of electrons within the Dirac cone so that it exists only in doped graphene. As mentioned above, the Fermi level is shifted upward by 0.05 eV. A more pronounced peak is visible (not shown here) if we artificially shift the Fermi level further up and introduce more electrons into the cone [34].

As q increases [see Fig. 2(b)], the π plasmon shifts to higher energy, similar to that in freestanding graphene. The height of the peak, however, changes only slightly and converges to that of freestanding graphene at around $q = 0.6/\text{Å}$. This suggests that the screening from the substrate gets weaker with increasing q.

Metallic substrate.—In contrast to semiconducting substrates, metallic substrates can sustain surface plasmons that can couple to the plasmons in graphene [21]. As we are not aware of any experiments on plasmon excitations of graphene on a metallic substrate, we consider Al(111) as a generic model for a free-electron-like metal. The system under study consists of a single layer of graphene on top of four Al (111) layers using a 1×1 unit cell. Graphene binds weakly to the Al surface with an (local-density approximation) interplane distance of 3.36 Å and binding energy per C atoms of 0.049 eV, in good agreement with van der Waals density-functional theory calculations [20]. As can be seen from the inset in Fig. 3, the Fermi level is shifted by around 0.5 eV above the Dirac cone of graphene, introducing slight electron doping into graphene.

The surface loss functions of graphene/Al are shown in Fig. 4. Although Al exhibits strong surface and bulk plasmonic excitations, these features are suppressed in the surface loss function calculated by using Eq. (5). The solid line indicates the graphene at the equilibrium distance from the surface. In contrast to the SiC semiconducting substrate, where the 5 eV peak still exists, the π plasmon is completely quenched by the Al substrate. Instead, a strong peak between 8 and 10 eV is visible in the spectrum. It arises from the collective excitations at the interface between graphene and Al [35].

Discussions.—The strong influence of the substrate on the plasmons may have two distinct origins: (i) the "static" effect, that is, the change of ground state wave functions due to hybridization with the states of the substrate and (ii) the "dynamical" effect, that is, the mutual dielectric screening between graphene and the substrate. In order to distinguish these two effects, we construct a model [36], shown as the inset in Fig. 4, separating the graphene (g) and substrate (s) into two subsystems that are connected with only Coulomb interaction and without any wave function overlap. The response function for each independent subsystem is χ^g and χ^s, respectively. In an applied external field δV_{ext}, the density response for each subsystems is written as

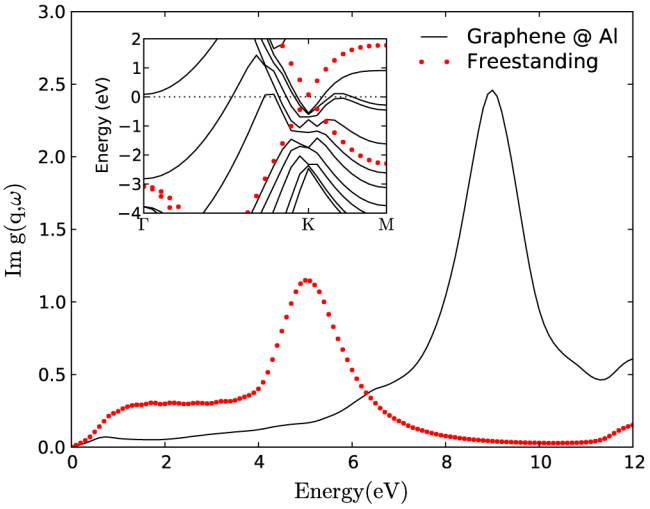

FIG. 3 (color online). Surface loss functions at $q = 0.046/\text{Å}$ and band structure (inset) for freestanding (red dots) and graphene on an Al substrate (black line).

$$\begin{aligned} \delta n^g &= \chi^g[\delta V_{\text{ext}} + V_c \delta n^s], \\ \delta n^s &= \chi^s[\delta V_{\text{ext}} + V_c \delta n^g], \end{aligned} \tag{5}$$

where V_c is the Coulomb interaction kernel. An effective response function for graphene can thus be defined as

$$\chi^g_{\text{eff}} = \frac{\delta n^g}{\delta V_{\text{ext}}} = \frac{\chi^g[1 + V_c \chi^s]}{1 - \chi^g V_c \chi^s V_c}. \tag{6}$$

A similar definition applies to the substrate χ^s_{eff}. The sum of χ^g_{eff} and χ^s_{eff} is the total response of the two subsystems within the model. Its difference with respect to the calculated *ab initio* response of the combined graphene-substrate (g/s) system is a measure of the hybridization between the two subsystems. As shown in Fig. 4, such differences are minimal for both SiC [(a)] and Al substrate [(b)], suggesting that the dynamical responses are dominated by Coulomb interactions. The slightly larger deviation observed for Al can be attributed to the shift of the Fermi level with respect to the Dirac cone of graphene shown in the inset in Fig. 3. This shift is not taken into account in the model calculation. The Coulomb interaction gets weaker with increasing q as it scales with $1/|\mathbf{q}|^2$, explaining the fact that the screening gets weaker and the strength of the plasmon recovers to that of freestanding graphene at large q. Finally, we note that the damping of the plasmon is very long ranged. Based on our EELS spectra for adsorption distances up to $d = 20$ Å, we deduce that the height of the π plasmon falls off slower than $1/d$.

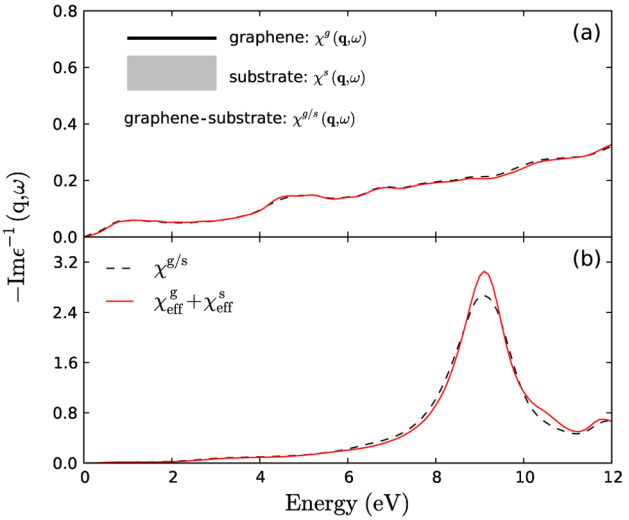

FIG. 4 (color online). Loss function of graphene/SiC (a) and graphene/Al (b). The *ab initio* results (black dashed line) are compared with that obtained from the sum of the effective response function of two subsystems (red solid line). Inset in (a): Illustration of the two independent subsystems: graphene and substrate with response function χ^g and χ^s, respectively.

In conclusion, the study of the interface and interactions between graphene and supporting substrates is crucial for large scale graphene-based applications. Our first-principles calculations show that the plasmons in graphene are significantly damped by a semiconducting substrate and completely quenched by a metallic substrate, in particular, in the long wavelength limit. The electronic response is dominated by the long ranged Coulomb interaction which makes the effect significant even for weakly coupled graphene-substrate systems. The strong damping of plasmons by the substrate needs to be taken into account in the future design of graphene-based materials for plasmonic applications.

One of the authors (J. Y.) acknowledges Marco Vanin, Jens Jørgen Mortensen, and Marcin Dułak for valuable discussions. The Center for Atomic-scale Materials Design is sponsored by the Lundbeck Foundation. The Catalysis for Sustainable Energy initiative is funded by the Danish Ministry of Science, Technology and Innovation. This work is partly supported by the Center on Nanostructuring for Efficient Energy Conversion (CNEEC) under DOE.

*thygesen@fysik.dtu.dk

[1] A. H. Castro Neto *et al.*, Rev. Mod. Phys. **81**, 109 (2009).
[2] C. Kramberger *et al.*, Phys. Rev. Lett. **100**, 196803 (2008).
[3] T. Eberlein *et al.*, Phys. Rev. B **77**, 233406 (2008).
[4] U. Bangert *et al.*, Phys. Status Solidi A **205**, 2265 (2008).
[5] J. Lu, K. P. Loh, H. Huang, W. Chen, and A. T. S. Wee, Phys. Rev. B **80**, 113410 (2009).
[6] T. Langer, H. Pfnür, H. W. Schumacher, and C. Tegenkamp, Appl. Phys. Lett. **94**, 112106 (2009).
[7] E. H. Hwang and S. Das Sarma, Phys. Rev. B **75**, 205418 (2007).
[8] Y. Liu, R. F. Willis, K. V. Emtsev, and T. Seyller, Phys. Rev. B **78**, 201403 (2008).
[9] A. Bostwick *et al.*, Science **328**, 999 (2010).
[10] P. E. Trevisanutto, C. Giorgetti, L. Reining, M. Ladisa, and V. Olevano, Phys. Rev. Lett. **101**, 226405 (2008).
[11] Y. Liu and R. F. Willis, Phys. Rev. B **81**, 081406 (2010).
[12] E. G. Mishchenko, A. V. Shytov, and P. G. Silvestrov, Phys. Rev. Lett. **104**, 156806 (2010).
[13] S. A. Maier, *Plasmonics: Fundamentals and Applications* (Springer, New York, 2007).
[14] J. Coraux, A. T. N'Diaye, C. Busse, and T. Michely, Nano Lett. **8**, 565 (2008).
[15] P. W. Sutter, J.-I. Flege, and E. A. Sutter, Nature Mater. **7**, 406 (2008).
[16] K. V. Emtsev *et al.*, Nature Mater. **8**, 203 (2009).
[17] F. Varchon *et al.*, Phys. Rev. Lett. **99**, 126805 (2007).
[18] A. Mattausch and O. Pankratov, Phys. Rev. Lett. **99**, 076802 (2007).
[19] P. A. Khomyakov *et al.*, Phys. Rev. B **79**, 195425 (2009).
[20] M. Vanin *et al.*, Phys. Rev. B **81**, 081408 (2010).
[21] N. J. M. Horing, Phys. Rev. B **80**, 193401 (2009).
[22] K. F. Allison, D. Borka, I. Radović, L. Hadžievski, and Z. L. Mišković, Phys. Rev. B **80**, 195405 (2009).
[23] S. L. Adler, Phys. Rev. **126**, 413 (1962).
[24] N. Wiser, Phys. Rev. **129**, 62 (1963).
[25] J. J. Mortensen, L. B. Hansen, and K. W. Jacobsen, Phys. Rev. B **71**, 035109 (2005).
[26] J. Enkovaara *et al.*, J. Phys. Condens. Matter **22**, 253202 (2010).
[27] P. E. Blöchl, Phys. Rev. B **50**, 17 953 (1994).
[28] V. M. Silkin, E. V. Chulkov, and P. M. Echenique, Phys. Rev. Lett. **93**, 176801 (2004).
[29] Z. Yuan and S. Gao, Comput. Phys. Commun. **180**, 466 (2009).
[30] J. Yan, J. J. Mortensen, K. W. Jacobsen, and K. S. Thygesen (to be published).
[31] The ground state calculations are carried out by using projector augmented wave potentials in the local density approximation. van der Waals exchange-correlation functionals [M. Dion, H. Rydberg, E. Schröder, D. C. Langreth, and B. I. Lundqvist, Phys. Rev. Lett. **92**, 246401 (2004); Phys. Rev. Lett. **95**, 109902 (2005)] have also been employed. Both exchange functionals give very similar binding energies and distances. A supercell containing 20 Å vacuum and an uniform grid spacing 0.2 Å is used. The sampling of the first Brillouin zone corresponds to 4096 and 1024 k points for a 1×1 and 2×2 unit cell of graphene, respectively. The local field effects are taken into account through the off-diagonal elements of the $\chi^0_{\mathbf{GG}'}$ matrix, which is expanded by using $\sim$500 $\mathbf{G}$ vectors.
[32] K. V. Emtsev, F. Speck, T. Seyller, L. Ley, and J. D. Riley, Phys. Rev. B **77**, 155303 (2008).
[33] A. G. Marinopoulos *et al.*, Phys. Rev. Lett. **89**, 076402 (2002).
[34] Y. Gao and S. W. Gao (private communication).
[35] The surface plasmon of the Al surface splits into a symmetric and an antisymmetric mode for the thin film we used; however, it does not change our conclusion that the π plasmons are completely quenched by the substrate.
[36] J. M. Pitarke *et al.*, Phys. Rev. B **70**, 205403 (2004).